J. Plasma Physics (2005), *vol.* 71, *part* 6, *pp.* 769–784. © 2005 Cambridge University Press
doi:10.1017/S0022377805003776 Printed in the United Kingdom

Nonlinear shielding of planar test charge in one-dimensional Vlasov–Poisson plasma

N. DAS[1] and H. SCHAMEL[2]

[1]Department of Physics, Tezpur University, Napaam-784 028, India
[2]Physikalisches Institut, Universitat Bayreuth, D-95440 Bayreuth, Germany

(Received 18 August 2004 and accepted 21 October 2004)

Abstract. The shielding of a one-dimensional, planar, permeable test charge has been studied theoretically. General expressions are derived and evaluated which show how the screening of a test charge, represented by the floating potential ψ, surface charge density q and screening length L, depends on various plasma parameters such as the temperature of electron and ions and particle streaming velocities. Particular attention has been given to analyzing the influence of particle trapping (reflection) in the charging and screening problem. No charging model can adequately describe the screening mechanism unless proper care is taken in choosing suitable distribution functions for both plasma species. In this paper, such a theory has been developed that provides the general idea about the charging of a grid in plasmas under different environments and conditions. As the main outcome we have found that the shielding of a non-propagating test charge is stronger, the larger the trapped ion population and the higher the temperature ratio T_e/T_i are. Flux equality in the case of a propagating test charge restricts the solubility of the shielding problem to non-Boltzmann electrons and to a weak ψ and q only. In the cold ion limit a lower bound for the ion streaming velocity is found than that predicted by Bohm's criterion.

1. Introduction

In plasma physics the screening of a test charge is considered to be one of the fundamental issues needed for an understanding of plasma dynamics. An example of its relevance is the ion drag force, which is generally considered to be the most prominent candidate for explaining the particle repulsion leading to voids in rf discharges [1]. Its magnitude is known to depend strongly on the value of the screening length [2], about which a controversial discussion appeared recently in the literature [3, 4].

When dust grains are present in plasma or when plasma is confined in a finite volume, a sheath is formed around the grain or near the walls of the chamber shielding these objects from the unperturbed plasma. This shielding depends upon the surrounding particles as well as on the particles trapped or reflected near the test charge or the wall. The trapped distribution of particles may hence have a drastic effect on the floating potential of the grain. Most of the work done on shielding so far, has ignored the effect of electron–ion trapping. The widely accepted and well-known charging model viz., orbital motion limited theory, does not consider electron–ion trapping in determining the charge of the grains.

https://doi.org/10.1017/S0022377805003776 Published online by Cambridge University Press

Electrostatic screening around a test charge finds applications in various fields ranging from physical to biological as well as chemical systems. A complete theory in this regard is still not available. The study of macro-ions and the screening around them is an interesting problem in biological, chemical as well as physical systems. Macro-ions are important in DNA, various cells and viruses, charged lipid membranes, charged solid particles, etc. [5]. The electrostatic energy between a DNA molecule and the histone octamer may be an interesting field of application in the study of screening around a test charge.

Elaborate studies have been made on the screening of a probe or a test charge in a plasma environment. The work was initiated by Langmuir in 1920 [6], and followed by many others in the subsequent years. Although orbital motion limited (OML) theory is widely accepted, it has its own limitations. Allen et al. showed in their paper [7] that OML theory is never satisfied in Maxwellian plasmas, even in the case of very small bodies, i.e. those with radii much smaller than the plasma Debye length.

Ion trapping was considered by Laframboise [8] and Al'pert et al. [9] in their theories of probes and spacecraft, respectively. Very recently Allen and Kennedy have presented a new analytical theory for charging small probes and dust where they have taken ion absorption into account [10].

In recent years, a lot of work has been done on shielding and charging of a grain in plasma, where trapping has been considered more seriously. Reimann and Fajans [11] discussed the significance of the trapping effect on the study of shielding. They also mentioned experiments that have demonstrated that the significant number of trapped particle density may result in a change of sign of the shielding. Lampe et al. [12] have made an analytical study of the shielding of a spherical charged particle in plasma, and have showed how the trapped ions built up around dust particles dominate the shielding process and result in a considerable increase in ion current to the grain and suppression of the floating potential. The trapped particles created by charge-exchange collisions may have an intense effect on the grain dynamics and interaction between two grains in plasma. A grain surrounded by a trapped ion cloud may behave like a classical atom, so van der Waals type attractive forces between grains may be important. In this respect, our planar sheet model is less elaborate as we neglect, for example, collisions or the three-dimensional (3D) nature of dust grains. In one dimension, on the other hand, the Vlasov solution can be found exactly, fitting to a thermal plasma, and hence no further approximations are necessary. As a result, interesting physical effects, such as the suppression of the floating potential in the case of streaming ions, can be found exactly in one dimension and are hence not due to 3D or other precious supplements. In this case our model provides a base towards which more sophisticated models can be tested.

2. Basic equations

A 1D planar, permeable test charge (sheet or grid) immersed in a collisionless thermal plasma is known to acquire in steady state a negative potential (floating potential). The associated electric field surrounding the test charge turns out to be attractive for ions and repulsive for electrons, such that an ion rich sheath is formed which screens the negative surface charge. A basic question, which to our knowledge has not yet been solved completely, is the dependence of sheath, test charge and screening length on the various plasma parameters, which include not

https://doi.org/10.1017/S0022377805003776 Published online by Cambridge University Press

only the thermal plasma parameters but also those that are due to the coherent structure, such as the trapping parameters. To be more exact, we first introduce dimensionless quantities:

$$x := \tilde{x}/\lambda_{\mathrm{D}}, \quad v := \tilde{v}/v_{\mathrm{the}}, \quad u := \tilde{u}/v_{\mathrm{thi}},$$

$$\phi := e\tilde{\phi}/kT_{\mathrm{e0}}, \quad \Theta := T_{\mathrm{eo}}/T_{\mathrm{io}}, \quad q := -\tilde{q}/e,$$

where the tilde denotes dimensional quantities [13]. For a grid (a penetrable sheet or test charge), the situation is shown in Figs. 1(a)–(c) showing the potential distribution, the electron phase space and the ion phase space, respectively. The potential $\phi(x)$ satisfies $-\psi \leqslant \phi(x) \leqslant 0$ in the wave frame (the frame in which the sheet is at rest) and its derivative jumps such that the surface charge density q is given by

$$q = \phi'(0^+) - \phi'(0^-) > 0. \tag{1}$$

It should be noted that $q > 0$ implies a negative surface charge density $\tilde{q} = -eq < 0$. In phase space, the trajectories are given by the contour lines of constant energy

$$\epsilon_{\mathrm{e}} := \frac{v^2}{2} - (\phi + \psi), \tag{2}$$

$$\epsilon_{\mathrm{i}} := \frac{u^2}{2} + \Theta\phi, \tag{3}$$

which are defined such that $\epsilon_s = 0, s = \mathrm{e}, \mathrm{i}$ describes the separatrix, the limiting lines that separate free from trapped particles.

We assume a Maxwellian state shifted by $-v_0$ ($-u_0$) at $x = 0$ ($x = \infty$), the locations where trapped electrons (ions) are absent, and hence solve the corresponding Vlasov equation by the ansatz [14],

$$f_{\mathrm{e}}(x, v) = \frac{\hat{A}}{\sqrt{2\pi}}[e^{-\frac{1}{2}(\sigma_{\mathrm{e}}\sqrt{2\epsilon_{\mathrm{e}}}+v_0)^2}\Theta(\epsilon_{\mathrm{e}}) + e^{-(\frac{1}{2}v_0^2+\beta\epsilon_{\mathrm{e}})}\Theta(-\epsilon_{\mathrm{e}})], \tag{4}$$

$$f_{\mathrm{i}}(x, u) = \frac{1}{\sqrt{2\pi}}[e^{-\frac{1}{2}(\sigma_{\mathrm{i}}\sqrt{2\epsilon_{\mathrm{i}}}+u_0)^2}\Theta(\epsilon_{\mathrm{i}}) + e^{-(\frac{1}{2}u_0^2+\alpha\epsilon_{\mathrm{i}})}\Theta(-\epsilon_{\mathrm{i}})]. \tag{5}$$

In (4) and (5), a number of parameters have been introduced that will finally affect the self-consistent solution of our charging and shielding problem, such as $\alpha(\beta)$, representing the status of trapped ions (electrons), the ion (electron) flux being proportional to $-u_0$ ($-v_0$) is given by $-u_0 v_{\mathrm{thi}}$ ($-\hat{A}v_0 v_{\mathrm{the}}$), and the temperature ratio Θ. Note that, in (4) and (5), $\Theta(\epsilon_s)$ is the Heaviside function, that σ_s, $s = \mathrm{e}, \mathrm{i}$, is the sign of the velocity and that $\hat{A}$ is a normalization constant, allowing quasi-neutrality at infinity. In Figs. 1(a)–(c) we have assumed a situation symmetric in x that demands equality of the asymptotic states (at $|x| = \infty$) and hence a flow of particles across the sheet such as for a sufficiently penetrable grid or an idealized emissive wall (which re-emits absorbed particles according to their incoming energy). This symmetry is lost in the case of a non-emissive wall sheet, in which case orbits at $x = 0$ with $u > 0$ ($v > 0$) are not occupied, giving rise to modifications of the results presented below.

Notice that the distributions (4) and (5) are continuous across the separatrix, a property being generally lost if the original Bernstein, Greene, Kruskal (BGK) method [15] for constructing electrostatic Vlasov–Poisson equilibria [13, 16] is used instead.

https://doi.org/10.1017/S0022377805003776 Published online by Cambridge University Press

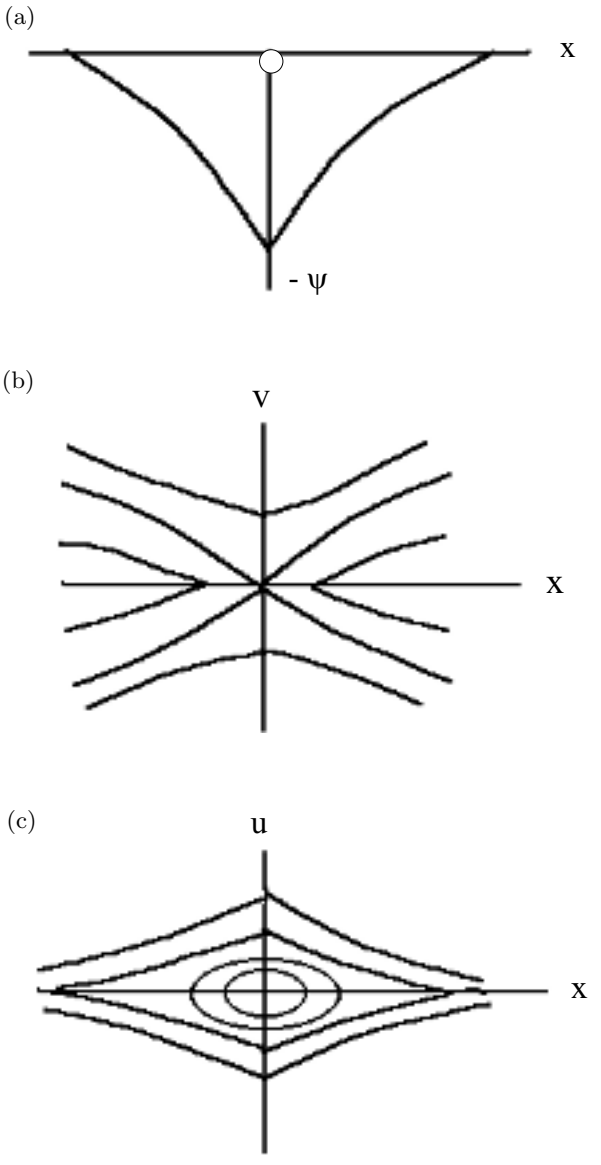


Figure 1. (a) Potential distribution, (b) electron phase space, (c) ion phase space.

Integrating the distributions (4) and (5) over the velocity we get the densities [13, 14, 17, 18]

$$n_{\mathrm{e}}(\phi) = \hat{A} e^{-v_0^2/2} \left[F\left(\frac{v_0^2}{2}, \phi + \psi \right) + T_{\pm}\left(\beta, \phi + \psi \right) \right], \tag{6}$$

$$n_{\mathrm{i}}(\phi) = e^{-u_0^2/2} \left[F\left(\frac{u_0^2}{2}, -\Theta\phi \right) + T_{\pm}\left(\alpha, -\Theta\phi \right) \right], \tag{7}$$

https://doi.org/10.1017/S0022377805003776 Published online by Cambridge University Press

where $F(T)$ represents the contribution from the free (trapped) particles and index $\pm$ in T_+ (T_-) holds for positive (negative) trapped particle parameters α and β, respectively. An outline of these functions is presented in the Appendix.

Self-consistency finally requires Poisson's equation

$$\phi''(x) = n_{\rm e}(\phi) + q\delta(x) - n_{\rm i}(\phi), \tag{8}$$

from which the jump condition (1) and $\phi(x)$ result. The latter satisfies for $x \neq 0$

$$\phi''(x) = n_{\rm e}(\phi) - n_{\rm i}(\phi) \equiv -V'(\phi), \tag{9}$$

where the 'classical' potential $V(\phi)$ has been introduced for convenience. A quadrature then yields the 'classical' energy, $\phi'(x)^2/2 + V(\phi) = 0$, from which, knowing $V(\phi)$, the potential $\phi(x)$ is obtained by inversion of

$$x = \int_{-\psi}^{\phi} \frac{d\varphi}{\sqrt{-2V(\varphi)}} \equiv x(\phi) \tag{10}$$

valid for $x \geqslant 0$. As a boundary condition we require quasineutrality at infinity: $n_{\rm e}(0) = n_{\rm i}(0) = 1$, which becomes, using $F(u_0^2/2, 0) = e^{-u_0^2/2}$ and $T_\pm(\alpha, 0) = 0$,

$$R := \hat{A}e^{-v_0^2/2} = \left[F\left(\frac{v_0^2}{2}, \psi\right) + T_\pm(\beta, \psi)\right]^{-1}. \tag{11}$$

By means of the 'classical' energy expression we then find for the associated surface charge density (1)

$$q = 2\sqrt{-2V(-\psi)}. \tag{12}$$

Generally speaking, $V(-\psi)$, will depend on various parameters and hence a variety of solutions is expected in dependency of these parameters.

Our main goal will be the determination of the normalized surface charge density $-q < 0$, the normalized grid potential $-\psi < 0$ and the shielding length of the sheath L surrounding the grid. As we will see, trapping, particle drifts (flows), temperatures as well as nonlinearity do have a profound impact on the solution and hence on the charging/shielding problem.

Before analyzing the result in more detail, we present the 'classical' potential in its full generality (assuming $V(0) = 0$):

$$\begin{aligned} -V(\phi) = R\left[H\left(\frac{v_0^2}{2}, 0, \phi + \psi\right) - H\left(\frac{v_0^2}{2}, 0, \psi\right) + P_\pm(\beta, \phi + \psi) - P_\pm(\beta, \psi)\right] \\ + \frac{1}{\Theta}e^{-u_0^2/2}\left[H\left(\frac{u_0^2}{2}, 0, -\Theta\phi\right) + P_\pm(\alpha, -\Theta\phi) - 1\right]. \end{aligned} \tag{13}$$

3. A test charge at rest in a plasma with Boltzmann electrons

To analyze the charge and the sheath of a grid (test charge) immersed in a plasma, we start with the simplest case. We consider additional physical effects, such as finite flows, later in Sec. 4.

Assuming a non-propagating test charge ($v_0 = 0 = u_0$) and isothermal electrons ($\beta = 1$) we get using (A 6),

$$-V(\phi) = e^\phi - 1 + \frac{1}{\Theta}\left[P_\pm(\alpha, -\Theta\phi) - 1\right] \tag{14}$$

and using (12),

$$q = 2\sqrt{2}\left\{e^{-\psi} - 1 + \frac{1}{\Theta}[P_\pm(\alpha, \Theta\psi) - 1]\right\}^{1/2}. \tag{15}$$

https://doi.org/10.1017/S0022377805003776 Published online by Cambridge University Press

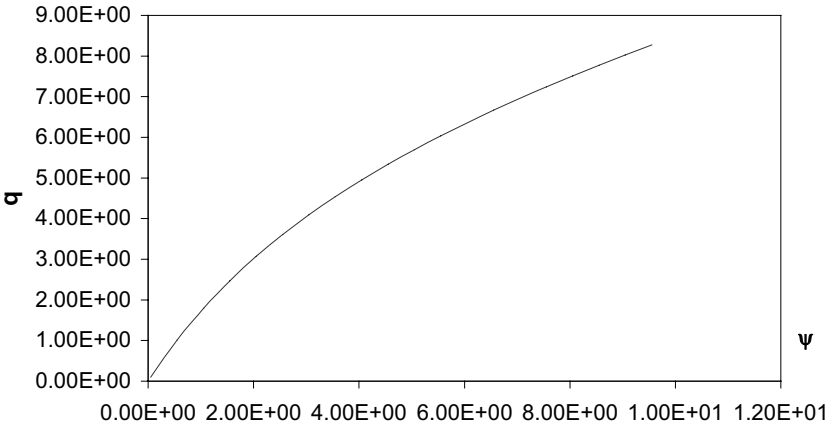


Figure 2. Plot of $q(\psi)$ for immobile ions.

This gives a three-parameter test charge that still depends on the temperature ratio Θ, on the depth ψ of the negative grid potential and on ion trapping, $q = q(\alpha, \Theta, \psi)$.

The simplest condition refers to that of the immobile ions ($m_\mathrm{i} \to \infty$), $n_\mathrm{i} \to 1$ which is achieved by letting $\Theta \to 0$. In this case (14) and (15) reduce with the help of (A 7) to

$$-V(\phi) = e^{\phi} - 1 - \phi, \tag{16}$$

$$q = 2\sqrt{2}\{e^{-\psi} - 1 + \psi\}^{1/2}. \tag{17}$$

The ion trapping effect is lost in this limit and we get from (17) a one-particle solution $q = q(\psi)$. Figure 2 shows that there is a monotonic relationship between q and ψ, i.e. between the surface charge density and the grid potential, which for small and large amplitudes, simplifies to

$$q = 2\psi, \quad \psi \ll 1 \quad \text{and} \quad q = 2\sqrt{2\psi}, \quad \psi \gg 1.$$

For mobile ions, we have to go back to (15) in which case $q = q(\alpha, \Theta, \psi)$, shows an additional temperature (Θ) and ion trapping (α) dependence. First we consider the θ and ψ dependence of q, keeping $\alpha = 1$ fixed, i.e. $q(1, \Theta, \psi)$, as shown in Fig. 3(a) for four values of θ. Analytically, it is found that

$$q = 2\psi\sqrt{1 + \Theta} \quad \text{for } \psi \ll 1,\ \Theta\psi \ll 1 \quad (\text{valid for any } \alpha)$$

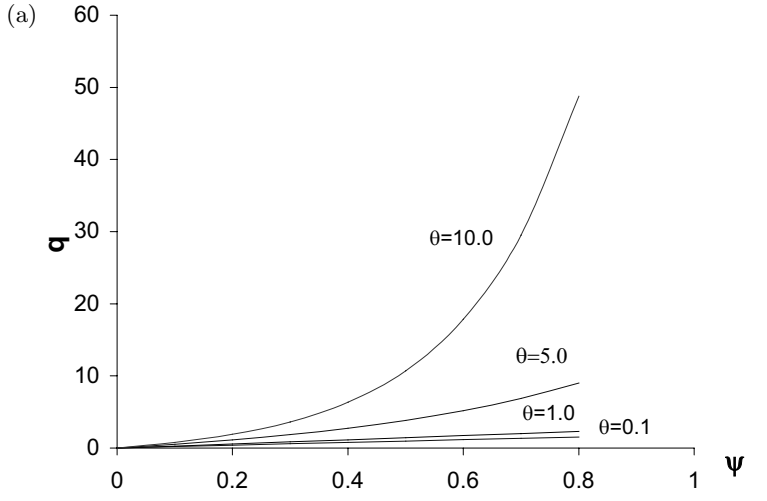
and that

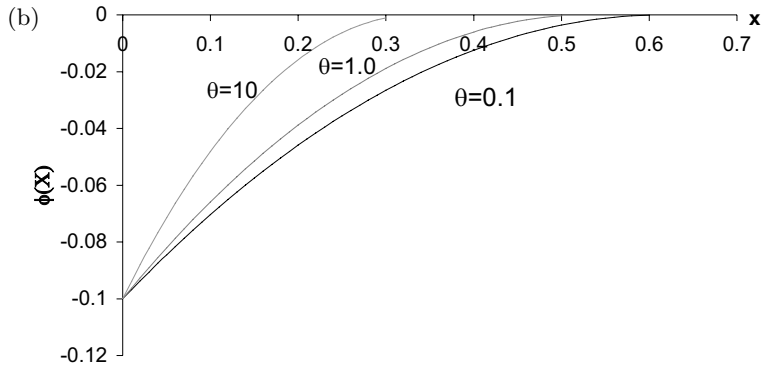
$$q = 2\sqrt{\frac{2}{\Theta}}e^{\Theta\psi/2} \text{ for } \psi \gg 1,\ \Theta\psi \gg 1$$

in agreement with Fig. 3(a). There is hence a strong Θ dependence of q, i.e. by lowering T_i (increase of Θ) at constant grid potential ψ, the surface charge density is intensified rather strongly.

The reason for this strong effect is recognized if we consider $\phi(x)$ for fixed $\psi = 0.1$, as obtained by inversion of (10), and plot it in Fig. 3(b) for three values of Θ. An increase of Θ by cooler ions is seen to narrow the sheath, i.e. to shorten the screening length, and to increase the electric field at the grid and hence q. In terms of the densities we can argue as follows. For isothermal electrons and a resting test charge

https://doi.org/10.1017/S0022377805003776 Published online by Cambridge University Press





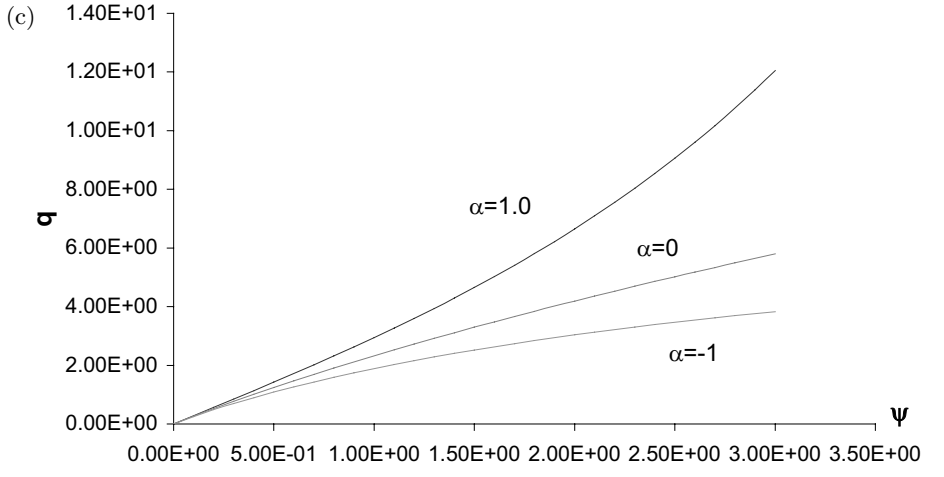


Figure 3. (a) Charge versus ψ for different θ; (b) ϕ versus x for $\theta = 0.1, 1.0, 10.0$; $\psi = -0.1$; (c) q versus ψ for $\theta = 1.0$, $\alpha = -1, 0, 1$; (d) charge versus α for $\theta = 1$, $\psi = 1.0$; (e) ψ versus x for $\alpha = -1, 0, 1$.

https://doi.org/10.1017/S0022377805003776 Published online by Cambridge University Press

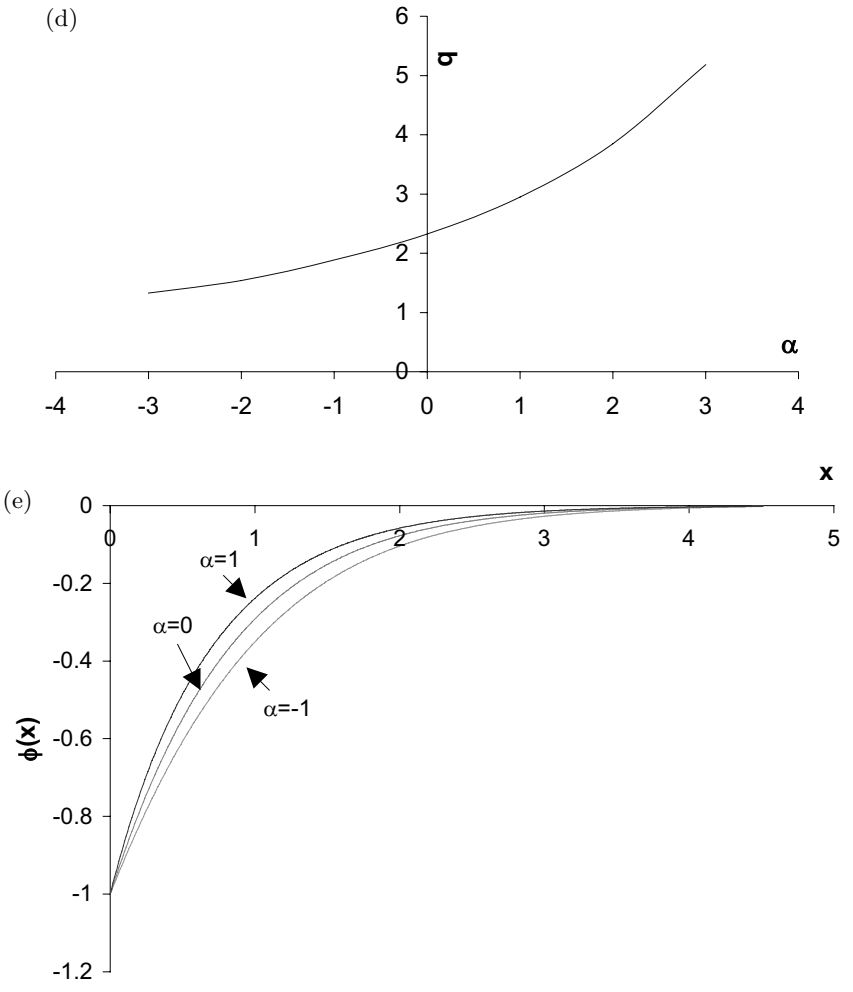


Figure 3. Continued.

we get from (6) and (7) using the formulas in the Appendix

$$n_{\mathrm{e}}(\phi) = e^{\phi}; \quad n_{\mathrm{i}}(\phi) = e^{-\Theta\phi} \tag{18}$$

valid for $\alpha = 1$, which are the usual Boltzmann expressions. For $\phi < 0$ the ion density always exceeds the electron density, giving rise to a net positive charge density and hence to a negative curvature of ϕ. An effective ion sheath surrounds and shields the grid in which the ion population dominates over the electron population. This dominance is the stronger the cooler the ions are and hence $|\phi|$ decays faster in x, yielding to a shorter normalized screening length, L.

To learn about the expected effect of ion trapping, we extend this consideration to arbitrary α, in which case we get

$$n_{\mathrm{e}}(\phi) = e^{\phi},$$

https://doi.org/10.1017/S0022377805003776 Published online by Cambridge University Press

$$n_{\rm i}(\phi) = I(-\Theta\phi) + \begin{cases} \dfrac{1}{\sqrt{\alpha}} e^{-\alpha\Theta\phi}\,\mathrm{erf}\sqrt{-\alpha\Theta\phi}, & \alpha \geqslant 0 \\ \dfrac{2}{\sqrt{\pi|\alpha|}} W(\sqrt{\alpha\Theta\phi}), & \alpha < 0. \end{cases} \tag{19}$$

The ion density expression $n_{\rm i}$ simplifies further if we assume small $|\Theta\phi| \ll 1$, in which case we get, using (A 7),

$$n_{\rm i}(\phi) = 1 - \Theta\phi - \frac{4}{3\sqrt{\pi}}(1-\alpha)(-\Theta\phi)^{3/2} + \cdots . \tag{20}$$

This expression shows that decreasing the amount of trapped ions by lowering α weakens the ion density and makes the shielding and charging process less effective, although it appears in the limit $\Theta\psi \ll 1$ only as a small correction, as long as $|\alpha| \sim \mathrm{O}(1)$. However, if the depletion of the ion distribution in the trapping range becomes very large such that the third term in (20) becomes comparable with the second term, namely when $-\alpha \sim (\Theta\psi)^{-1/2} \gg 1$, the sheath is going to lose its ionic character and the shielding/charging effect declines. Figure 3(c) shows the ψ dependence of $q(\alpha, 1, \psi)$ for $\Theta = 1$ and three values of α, Fig. 3(d) the α-dependence of $q(\alpha, 1, 1)$ for $\Theta = 1 = \psi$ and Fig. 3(e) the space dependence of $\phi(x)$ for three values of α. One recognizes a strong decline of the surface charge density with an increasing deficit of trapped ions, i.e. when α becomes smaller and negative.

A similar effect, namely a drastic increase of the shielding length L, is observed if the trapped ion range is continuously depleted.

We conclude that the ion temperature has a strong impact, but the most pronounced effect on the charging/shielding of a grid (test charge) being at rest in a plasma, results from ion trapping. The less occupied the trapped ion range is, the less (larger) is the surface charge density (screening length).

Next we study the effect of a moving grid, respectively a propagating test charge.

4. A moving grid in a plasma with non-Boltzmann electrons

When the test charge is propagating with the actual velocity $\tilde{v_0}$, we have $\tilde{v_0} = v_0 v_{\rm the} = u_0 v_{\rm thi}$, expressing merely the common frame of reference. Hence it holds that $u_0 = \mu v_0$ with

$$\mu = v_{\rm the}/v_{\rm thi} = \sqrt{\frac{m_{\rm i}}{m_{\rm e}}\frac{T_{\rm e0}}{T_{\rm i0}}} = \sqrt{\Theta/\delta},$$

where $\delta = m_{\rm e}/m_{\rm i}$ is the small mass ratio. Since μ is typically large, the main effect of a streaming plasma will come from u_0. Demanding, furthermore, equality of fluxes across the sheet to maintain a stationary surface charge density, we get $\hat{A} = 1$ in (6) and (11), providing an internal relationship among the (electronic) parameters v_0, β and ψ, given by

$$R = e^{-v_0^2/2} = \left[F\left(\frac{v_0^2}{2}, \psi\right) + T_{\pm}(\beta, \psi)\right]^{-1}. \tag{21}$$

The reason is clear. At infinity, where $n_{\rm i} = 1$, we have a shifted Maxwellian for the ions yielding the ion flux $-u_0 v_{\rm thi}$; the electron distribution, on the other hand, exhibits a maximum trapping width in velocity $\triangle v = 2\sqrt{2\psi}$. This implies that all the parameters v_0, β and ψ are involved to get $n_{\rm e}(0) = 1$. Moreover, using flux

https://doi.org/10.1017/S0022377805003776 Published online by Cambridge University Press

conservation, we can determine its value at $x = 0$ or $\phi = -\psi$, in which case we get $-v_0 v_{\rm the} n_{\rm e}(-\psi) \equiv -v_0 v_{\rm the} \hat{A}$. But the latter expression has to be $-v_0 v_{\rm the}$, which means $n_{\rm e}(-\psi) = 1$ and hence $\hat{A} = 1$. Equal fluxes therefore imply $n_{\rm e}(0) = 1 = n_{\rm e}(-\psi)$.

By this additional constraint stemming from flux conservation, we therefore get for the electron density

$$n_{\rm e}(\phi) = \frac{F(v_0^2/2, \phi + \psi) + T_{\pm}(\beta, \phi + \psi)}{F(v_0^2/2, \psi) + T_{\pm}(\beta, \psi)}, \tag{22}$$

which satisfies $n_{\rm e}(0) = 1 = n_{\rm e}(-\psi)$. In contrast to $n_{\rm e}(\phi) = e^{\phi}$ of the previous chapter, which is monotonously decreasing as ϕ approaches $-\psi$, the new density (22) is no longer monotonic in ϕ and it first increases and later increases again, when ϕ approaches $-\psi$. It is clear that such behavior cannot be established within $\beta > 0$; the trapped electron range at $|x| = \infty (\phi = 0)$ must be excavated sufficiently to allow a density increase and subsequent decrease as one approaches the grid, due to the free electrons that must be populated sufficiently strongly already at $|x| = \infty$.

To see this further, let us discuss the constraint (21) for electrons in more detail.

First we consider the limit of a small grid potential, $\psi \ll 1$. In this case (21) becomes, using the appropriate Taylor expansion found in the Appendix,

$$-\frac{1}{2} Z_{\rm r}'(v_0/\sqrt{2}) = \frac{4}{3} b(\beta, v_0) \sqrt{\psi}, \tag{23}$$

which relates v_0, β and ψ. It constitutes a kind of nonlinear dispersion relation like that in the solitary electron hole propagation in plasmas with non-isothermal electrons [13, 19], as long as the right-hand side of (23) is small, v_0 is found in the thermal electron range, $v_0 \sim 1.3$, and hence is unrealistically large. To get smaller values of v_0, e.g. $v_0 \leqslant \sqrt{\delta} \ll 1$, valid for $u_0 \sim \sqrt{\Theta}$, i.e. for an ion flow velocity not exceeding the ion sound speed appreciably, the right-hand side of (23) must approach unity which implies

$$-\beta = \frac{3}{4} \sqrt{\pi/\psi} \gg 1. \tag{24}$$

The trapped electron range must be excavated. If we ask for large ψ, $\psi \gg 1$, then again (21) can be solved only for $\beta < 0$, in which case we would in addition get $v_0^2 = 2 \ln(|\beta| \sqrt{\pi \psi})$, being again too large.

Hence, the additional constraint (21) together with the demand of realistic velocities, $v_0 \leqslant \sqrt{\delta} \ll 1$, is met only for small grid potentials, $\psi \ll 1$, and electrons characterized by a notch in the trapped particle range with β given by (24).

Within this limit, namely $v_0 \leqslant \sqrt{\delta}$, $\psi \ll 1$ and $-\beta$ given by (24), the electron density expression (22) simplifies to

$$n_{\rm e}(\phi) \approx 1 + (\phi + \psi) - \frac{1}{\sqrt{\psi}} (\phi + \psi)^{3/2} + O(\delta, \psi^{3/2}). \tag{25}$$

Note, that the second and third terms on the right-hand side of (25) are of equal strength, and that $n_{\rm e}(0) \approx 1 \approx n_{\rm e}(-\psi)$ holds, as it should. For $\phi = -\psi/2$ we have $n_{\rm e}(-\psi/2) = 1 + 0.15\psi > 1$.

https://doi.org/10.1017/S0022377805003776 Published online by Cambridge University Press

The classical potential associated with (25) and including the full ion expression then reads, in the limit $\psi \ll 1, \Theta\psi \ll 1$,

$$-V(\phi) = \frac{(\phi+\psi)^2}{2}\left[1 - \frac{4}{5}\sqrt{\frac{\phi+\psi}{\psi}} + \cdots\right] - \frac{\psi^2}{10} + \phi\left[\frac{1}{4}Z_r'\left(\frac{u_0}{\sqrt{2}}\right)(-\Theta\phi) + \frac{8}{15}b(\alpha,u_0)(-\Theta\phi)^{3/2} + \cdots\right]. \tag{26}$$

It satisfies $-V(0) = 0$. For $\phi = -\psi$ we get

$$-V(-\psi) = \frac{\Theta\psi^2}{2}\left[-\frac{1}{2}Z_{\rm r}'(\mu_0/\sqrt{2}) - \frac{16}{15}b(\alpha,\mu_0)\sqrt{\Theta\psi} - \frac{1}{5\Theta}\right],$$

which should be positive to yield via (12) a non-vanishing surface charge density q. We get

$$q = 2\psi\sqrt{\Theta}\left[-\frac{1}{2}Z_{\rm r}'(\mu_0/\sqrt{2}) - \frac{16}{15}b(\alpha,\mu_0)\sqrt{\Theta\psi} - \frac{1}{5\Theta}\right]^{1/2}. \tag{27}$$

Hence, q is itself a small quantity, being dependent on μ_0, α, Θ and ψ. Figures 4(a) and 4(b) show that for $\psi = 0.01, \theta = 1, \alpha = 1$, a solution for q can be obtained only for u_0 up to 1.13. Beyond this value, y becomes negative and no solution can be obtained.

To see if and when a solution exists with dependence on α and u_0, we select $\Theta = 1$, $\psi = 10^{-2}$ and get as an existence condition

$$\alpha + u_0^2 - 1 > e^{u_0^2/2}\frac{15\sqrt{\pi}}{16}10\left[0.2 + \frac{1}{2}Z_{\rm r}'(u_0/\sqrt{2})\right],$$

from which we find for $u_0 = 0, 1.307, 2.12$, the inequality $\alpha > -12.28, 7.1, 319.4$. Hence for moderate $\alpha \leqslant 1$ (including a Boltzmann-like ion distribution) only velocities u_0 less than unity are admitted.

Of special interest is the cold ion limit, $\Theta \to \infty$, in which case, using the asymptotic formulas for F (I and K given in the Appendix), the ion density (7) becomes

$$n_{\rm i}(\phi) = \frac{1}{\sqrt{1 - 2\phi/U_0^2}} \simeq 1 + \frac{\phi}{U_0^2} + \cdots,$$

where U_0 is a quantity say of O(1) and $u_0 = \sqrt{\Theta}U_0 \to \infty$ holds. In this limit, there is no contribution from the trapped ions.The classical potential then becomes

$$-V(\phi) = \frac{(\phi+\psi)^2}{2}\left[1 - \frac{4}{5}\sqrt{\frac{\phi+\psi}{\psi}}\right] - \frac{\psi^2}{10} - \phi\left(1 + \frac{\phi}{2U_0^2}\right), \tag{28}$$

which is valid for $1 \ll \Theta\psi,\ 0 < \psi \ll 1$. It becomes at the grid, where $\phi = -\psi$,

$$-V(-\psi) = -\frac{\psi^2}{10} + \psi\left(1 - \frac{\psi}{2U_0^2}\right) = \psi - \frac{\psi^2}{2}\left(\frac{1}{5} + \frac{1}{U_0^2}\right), \tag{29}$$

which is unconditionally positive. If we had kept Boltzmann electrons in (28) instead, $n_{\rm e}(\phi) = e^{\phi}$, we would obtained in the $\psi \ll 1$ limit,

$$-V(\phi) = \frac{\phi^2}{2}(1 - U_0^{-2})$$

and the requirement of $-V(\phi) > 0$ would have introduced the inequality

$$U_0^2 \geqslant 1, \quad \tilde{u_0} \geqslant c_s^2, \tag{30}$$

https://doi.org/10.1017/S0022377805003776 Published online by Cambridge University Press

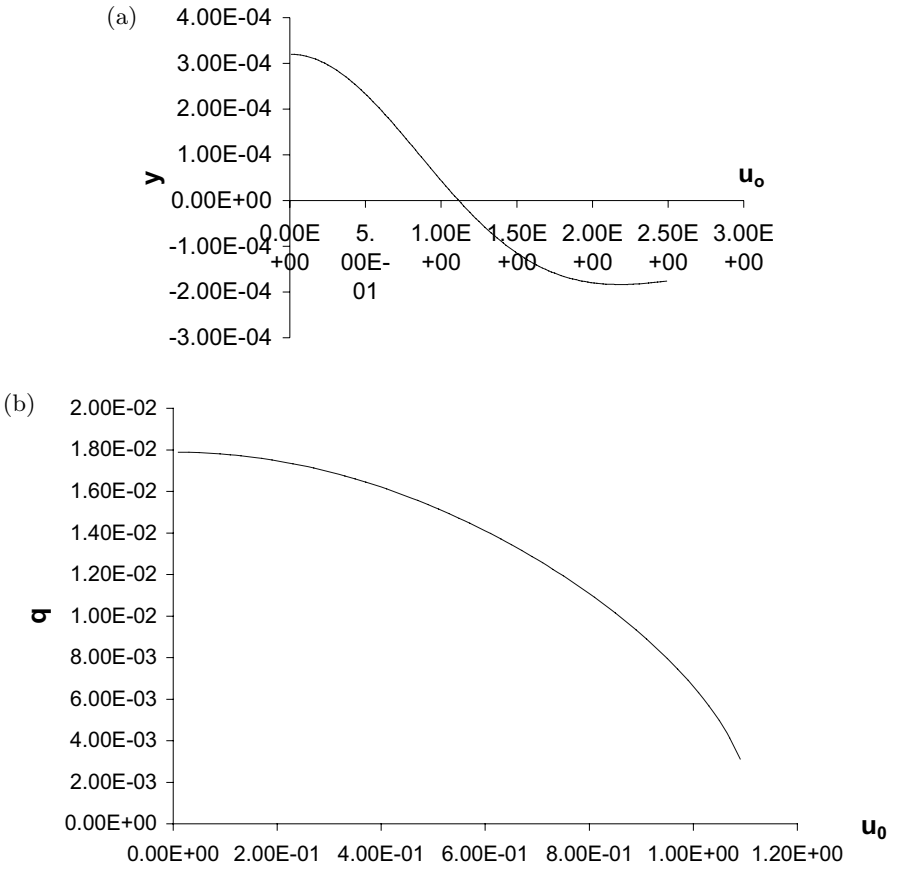


Figure 4. (a) $y = -V(-\psi)$ versus u_0 for $\theta = 1.0$, $\alpha = 1.0$, $\psi = 0.01$; charge q can be determined only up to $u_0 = 1.13$; (b) q versus u_0 for $\psi = 0.01$, $\theta = 1$, $\alpha = 1$; q can be determined up to $u_0 = 1.13$.

which is nothing else but Bohm's criterion. In our case, however, of a non-Boltzmann electron distribution, depressed in the trapped region, a sheath solution is formed for a much smaller bound on U_0 : $\sqrt{\psi/2} < U_0$.

The surface charge density q becomes, using (12),

$$q = 2\sqrt{2\psi}\left[1 - \frac{\psi}{2}\left(\frac{1}{5} + \frac{1}{U_0^2}\right)\right]^{1/2},$$

which is $\mathrm{O}(\sqrt{\psi})$ and hence an order of magnitude larger than for the warm ion result (27).

Our basic conclusion, therefore, is that kinetic electrons, with a deficit of electrons in the trapped region, favor sheath solutions for a permeable test charge allowing much lower ion drift velocities than those proposed by Bohm's criterion. However, the flux equality restricts the floating potential to small values, $\psi \ll 1$.

5. Summary and conclusion

The screening of test charge in plasma is a very rich theory and is a function of various plasma parameters such as particle velocity, trapping parameter, temperature

https://doi.org/10.1017/S0022377805003776 Published online by Cambridge University Press

of the species, etc. In this problem, an effort has been made to show the importance of trapping in the process of screening of a test charge. For this, Vlasov equation is solved by Schamel's distribution functions [14]. From the very beginning, it is assumed that the electron and ion distribution functions consist of both free and trapped parts. It is seen from the analysis that, for a stationary grid, the amount of trapped ions strongly affects the ion density and hence the shielding and charging process. The surface charge density q decreases rapidly with an increasing deficit of trapped ions. At the same time, the shielding length increases significantly when the trapped ion range is depleted gradually. Besides trapping, the temperature of electrons and ions also plays a major role in controlling the charging mechanism. A reduction in ion temperature results in the constriction of the sheath region and an increase in the surface charge density.

A detailed study has also been made regarding surface charge density for a test charge that is moving in plasma. In this case a new qualitative constraint is introduced by the demand of flux equality. One significant result is that trapped electrons range far away from the grid ($|x| = \infty, \phi = 0$) must be excavated sufficiently. Equality of the fluxes across the sheet and the demand of a realistic velocity $v_0 \leqslant \sqrt{\delta} \ll 1$ allows only a small grid potential $\psi \ll 1$, or, in other words, only a suppressed floating potential [12] and an electron distribution that is excavated, showing a notch in the distribution function. A drastic change is observed for Bohm's criterion in the cold ion limit ($\theta \longrightarrow \infty$) with a non-Boltzmannian electron distribution which is depressed in the trapped region. The sheath solution is found for a much smaller bound and the ion drift velocity may be much lower than that allowed by the Bohm criterion.

Appendix A. Definitions and properties of Schamel's functions

In this Appendix we define the functions used to express the densities and the 'classical' potential, as introduced by Schamel in [14, 17]. (The variable ϕ is considered here as a general variable, like x, satisfying $0 \leqslant \phi$.) The following hold:

$$F\left(\frac{v_0^2}{2}, \phi\right) := I(\phi) + K\left(\frac{v_0^2}{2}, \phi\right) \tag{A 1}$$

$$T_{\pm}(\beta, \phi) := \begin{cases} \dfrac{1}{\sqrt{\beta}} e^{\beta\phi} \operatorname{erf}\sqrt{\beta\phi}, & \beta \geqslant 0 \\ \dfrac{2}{\sqrt{\pi \mid \beta \mid}} W(\sqrt{\mid \beta \mid \phi}), & \beta < 0 \end{cases} \tag{A 2}$$

$$H\left(\frac{v_0^2}{2}, 0, \phi\right) := \int_0^{\phi} d\varphi\, K\left(\frac{v_0^2}{2}, \varphi\right) \tag{A 3}$$

$$\begin{aligned} P_{\pm}(\beta, \phi) &= \int_0^{\phi} I(\varphi)\, d\varphi + \int_0^{\phi} T_{\pm}(\beta, \varphi)\, d\varphi + 1 \\ &= I(\phi) + 2\sqrt{\frac{\phi}{\pi}}\left(1 - \frac{1}{\beta}\right) + \frac{1}{\beta\sqrt{\beta}} \begin{cases} e^{\beta\phi} \operatorname{erf}\sqrt{\beta\phi}, & \beta \geqslant 0 \\ \dfrac{2}{\sqrt{\pi}} W(\sqrt{\mid \beta \mid \phi}), & \beta < 0, \end{cases} \end{aligned} \tag{A 4}$$

https://doi.org/10.1017/S0022377805003776 Published online by Cambridge University Press

where we define

$$I(\phi) := e^{\phi}\,\mathrm{erfc}\sqrt{\phi}$$

$$K\left(\frac{v_0^2}{2},\phi\right) := \sqrt{\frac{2}{\pi}}\int_0^{\pi/2} d\varphi\, v_0\cos\varphi\exp\left[-\phi\tan^2\varphi+\frac{v_0^2}{2}\cos^2\varphi\right]\mathrm{erf}\left(\sqrt{\frac{v_0^2}{2}}\cos\varphi\right)$$

$$W(x) := e^{-x^2}\int_0^x dt\, e^{t^2}\quad\text{(Dawson function).} \tag{A 5}$$

The following holds:

$$\begin{gathered}
K(0,\phi)=0\\
K\left(\frac{v_0^2}{2},0\right)=e^{v_0^2/2}-1\\
H\left(\frac{v_0^2}{2},0,0\right)=0\\
H(0,0,\phi)=0\\
P_+(1,\phi)=e^{\phi}\\
P_{\pm}(0,\phi)=I(\phi)+2\sqrt{\frac{\phi}{\pi}}\left(1+\frac{2}{3}\phi\right)\\
P_-(-1,\phi)=I(\phi)+4\sqrt{\frac{\phi}{\pi}}-\frac{2}{\sqrt{\pi}}W(\sqrt{\phi}).
\end{gathered} \tag{A 6}$$

For small arguments, $\phi\ll 1$, the following expressions can be used:

$$\begin{gathered}
\mathrm{erf}(\phi)=\frac{2}{\sqrt{\pi}}\phi\left(1-\frac{\phi^2}{3}+\frac{\phi^4}{10}+\cdots\right)\\
I(\phi)=1-\frac{2}{\sqrt{\pi}}\sqrt{\phi}+\phi-\frac{4}{3\sqrt{\pi}}\phi^{3/2}+\frac{\phi^2}{2}+\cdots\\
W(\phi)=\phi\left(1-\frac{2}{3}\phi^2+\frac{4}{15}\phi^4+\cdots\right)\\
P_{\pm}(\beta,\phi)=1+\phi+\frac{\phi^2}{2}+\frac{8}{15\sqrt{\pi}}\beta\phi^{5/2}+\cdots,\quad\beta\text{ arbitrary}\\
T_{\pm}(\beta,\phi)=2\sqrt{\frac{\phi}{\pi}}\left(1+\frac{2}{3}\beta\phi+\frac{4}{15}(\beta\phi)^2+\cdots\right),\quad\beta\text{ arbitrary},\phi\ll 1\\
\text{or }\phi\text{ arbitrary},|\,\beta\,|\ll 1.
\end{gathered} \tag{A 7}$$

https://doi.org/10.1017/S0022377805003776 Published online by Cambridge University Press

For large arguments, $\phi \gg 1$, we instead have

$$\mathrm{erf}(\phi) = 1 - \frac{e^{-\phi^2}}{\sqrt{\pi}\phi}\left(1 - \frac{1}{2\phi^2} + \cdots\right) \approx 1$$

$$I(\phi) = \frac{1}{\sqrt{\pi\phi}}\left(1 - \frac{1}{2\phi} + \cdots\right)$$

$$W(\phi) = \frac{1}{2\phi}\left(1 + \frac{1}{2\phi^2} + \cdots\right)$$

$$P_+(\beta,\phi) = \frac{1}{\beta^{3/2}} e^{\beta\phi}, \quad \beta > 0,\ \beta\phi \gg 1 \tag{A 8}$$

$$P_\pm(0,\phi) = \frac{4}{3\sqrt{\pi}}\phi^{3/2}, \quad \beta \equiv 0$$

$$P_-(\beta,\phi) = \frac{2}{\sqrt{\pi}}\sqrt{\phi}\left(1 - \frac{1}{\beta}\right), \quad \beta < 0,\ |\beta|\phi \gg 1$$

$$K\left(\frac{v_0^2}{2},\phi\right) = \frac{\mathrm{erf}(v_0/\sqrt{2})e^{v_0^2/2}}{\sqrt{1 + 2\phi/v_0^2}}.$$

Furthermore, we have for small ϕ

$$F\left(\frac{v_0^2}{2},\phi\right) + T_\pm(\beta,\phi) = e^{v_0^2/2}\left\{1 - \frac{1}{2}Z_{\mathrm{r}}'\left(\frac{v_0}{\sqrt{2}}\right)\phi - \frac{4}{3}b(\beta,v_0)\phi^{3/2} + \cdots\right\} \tag{A 9}$$

$$H\left(\frac{v_0^2}{2},0,\phi\right) + P_\pm(\beta,\phi) - 1 = \phi\, e^{v_0^2/2}\left\{1 - \frac{1}{4}Z_{\mathrm{r}}'\left(\frac{v_0}{\sqrt{2}}\right)\phi - \frac{8}{15}b(\beta,v_0)\phi^{3/2} + \cdots\right\} \tag{A 10}$$

$$K\left(\frac{v_0^2}{2},\phi\right) = (e^{v_0^2/2} - 1) - \left[1 + \frac{1}{2}Z_{\mathrm{r}}'\left(\frac{v_0}{\sqrt{2}}\right)e^{v_0^2/2}\right]\phi + \frac{4v_0^2}{3\sqrt{\pi}}\phi^{3/2},\ \phi \ll 1 \tag{A 11}$$

$$K\left(\frac{v_0^2}{2},\phi\right) = \frac{v_0^2}{2}\left(1 + \frac{v_0^2}{4} - \phi + \cdots\right), \quad \text{for } v_0^2/2 \ll 1,\ \phi \ll 1, \tag{A 12}$$

where

$$\begin{aligned} -\frac{1}{2}Z_{\mathrm{r}}'\left(\frac{v_0}{\sqrt{2}}\right) &:= 1 - \sqrt{2}v_0 W(v_0/\sqrt{2}) \\ b(\beta,v_0) &:= \frac{1}{\sqrt{\pi}}(1 - \beta - v_0^2)e^{-v_0^2/2}. \end{aligned} \tag{A 13}$$

Note that Z_{r} stands for the real part of the complex plasma dispersion function.

References

[1] Samsonov, D. and Goree, J. 1999 *Phys Rev* E **59**, 1047.

[2] Barnes, M. S., Keller, J. H., Forster, J. C., O'Neil, J. A. and Coultas, D. K. 1992 *Phys. Rev. Lett.* **68**, 313.

https://doi.org/10.1017/S0022377805003776 Published online by Cambridge University Press

[3] Zafiu, C., Melzer, A. and Piel, A. 2002 *Phys. Plasmas* **9**, 4794; 2003 *Phys. Plasmas* **10**, 1278.
[4] Khrapak, S. A. *et al*. 2003 *Phys. Plasmas* **10**, 4579.
[5] Grosberg, A. YU., Nguyen, T. T. and Shklovskii, B. I. *Rev. Mod. Phys.* **74**, 2002.
[6] Allen, J. E., Boyd, R. L. and Reynolds, P. 1957 *Proc. Phys. Soc. London* B **70**, 297.
[7] Allen, J. E., Annaratone, B. M. and Angelis, U. de 2000 *Plasma Physics* **63**(4), 299–309.
[8] Laframboise, J. G. 1966 University of Toronto Institute for Aerospace Studies. Report No. 100.
[9] Al'pert, Y. L., Gurevich, A. V. and Pitaevskii, L. P. 1965 *Space Physics with Artificial Satellites*. New York: Consultants Bureau, ch. 8.
[10] Kennedy, R. V. and Allen, J. E. 2003 *J. Plasma Phys.* **69**, 485.
[11] Reimann, A. B. and Fajans, J. 1999 *Phys. Lett.* A **258**, 145.
[12] Lampe, M., Goswami, R., Sternovsky, Z., Robertson, S., Gavrishchaka, V., Ganguli, G. and Joyce, G. 2003 *Phys. Plasmas* **10**, 1500.
[13] Schamel, H. 2000 *Phys. Plasmas* **7**, 12.
[14] Schamel, H. 1972 *Plasma Phys.* **14**, 905.
[15] Bernstein, I. B., Greene, J. M. and Kruskal, M. D. 1957 *Phys. Rev.* **108**, 546.
[16] Schamel, H. 1975 *J. Plasma Phys.* **13**, 139.
[17] Schamel, H. 1971 *Plasma Phys.* **13**, 491.
[18] Schamel, H. 1986 *Phys. Rep.* **140**, 161.
[19] Schamel, H. 1979 *Physica Scripta.* **20**, 336.

https://doi.org/10.1017/S0022377805003776 Published online by Cambridge University Press